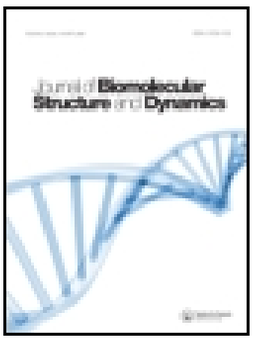

Journal of Biomolecular Structure and Dynamics

ISSN: 0739-1102 (Print) 1538-0254 (Online) Journal homepage: http://www.tandfonline.com/loi/tbsd20

Unravelling the Binding Mechanism and Protein Stability of Human Serum Albumin while Interacting with Nefopam Analogues: A Biophysical and Insilco approach

Mahesh Gokara, Vidadala V. Narayana, Vineet Sadarangani, Shatabdi Roy Chowdhury, Sreelaxmi Varkala, Dhevalapally B. Ramachary & Rajagopal Subramanyam

To cite this article: Mahesh Gokara, Vidadala V. Narayana, Vineet Sadarangani, Shatabdi Roy Chowdhury, Sreelaxmi Varkala, Dhevalapally B. Ramachary & Rajagopal Subramanyam (2016): Unravelling the Binding Mechanism and Protein Stability of Human Serum Albumin while Interacting with Nefopam Analogues: A Biophysical and Insilco approach, Journal of Biomolecular Structure and Dynamics, DOI: 10.1080/07391102.2016.1216895

To link to this article: http://dx.doi.org/10.1080/07391102.2016.1216895

Accepted author version posted online: 25 Jul 2016.
Published online: 25 Jul 2016.

Publisher: Taylor & Francis

Journal: *Journal of Biomolecular Structure and Dynamics*

DOI: http://dx.doi.org/10.1080/07391102.2016.1216895

Unravelling the Binding Mechanism and Protein Stability of Human Serum Albumin while Interacting with Nefopam Analogues: A Biophysical and *Insilco* approach

Mahesh Gokara[†], Vidadala V. Narayana[‡], Vineet Sadarangani[†], Shatabdi Roy Chowdhury[†], Sreelaxmi Varkala[†], Dhevalapally B.Ramachary[‡], Rajagopal Subramanyam[§*]

[†] Department of Biochemistry, School of Life Sciences, University of Hyderabad, Hyderabad 500046, India

[‡]School of Chemistry, University of Hyderabad, Hyderabad 500046, India

[§]Department of Plant Sciences, School of Life Sciences, University of Hyderabad, Hyderabad 500046, India

*Corresponding author

Rajagopal Subramanyam
Department of Plant Sciences
School of Life Sciences
University of Hyderabad 500 046 India
Tel: +91-40-23134572
Fax: +91-40-23010120
Email: srgsl@uohyd.ernet

Abstract

In this study, molecular binding affinity was investigated for Nefopam analogues (NFs), a functionalized benzoxazocine, with human serum albumin (HSA), a major transport protein in the blood. Its binding affinity and concomitant changes in its conformation, binding site and simulations were also studied. Fluorescence data revealed that the fluorescence quenching of HSA upon binding of NFs analogues is based on a static mechanism. The three analogues of NFs binding constants (K_A) are in the order of NF3>NF2>NF1 with values of $1.53 \pm 0.057 \times 10^4$, $2.16 \pm 0.071 \times 10^4$ and $3.6 \pm 0.102 \times 10^5$ M^{-1}, respectively. Concurrently, thermodynamic parameters indicate that the binding process was spontaneous, and the complexes were stabilized mostly by hydrophobic interactions, except for NF2 has one hydrogen bond stabilizes it along with hydrophobic interactions. Circular dichroism studies revealed that there is a decrease in α-helix with an increase in β-sheets and random coils signifying partial unfolding of the protein upon binding of NFs, which might be due to the formation of NFs-HSA complexes. Further, molecular docking studies showed that NF1, NF2 and NF3 bound to subdomain IIIA, IB and IIA through hydrophobic interactions. However, NF1 have additionally formed a single hydrogen bond with LYS 413. Furthermore, molecular simulations unveiled that NF's binding was in support with the structural perturbation observed in circular dichroism, which is evident from the RMSD and Rg fluctuations. We hope our insights will provide ample scope for engineering new drugs based on the resemblances with NFs for enhanced efficacy with HSA.

Keywords: human serum albumin, binding studies, nefopam, protein stability, docking studies

1. Introduction

Studies on the interaction between drugs and human serum albumin (HSA) have been a subject of interest in therapeutic drug monitoring. It has a significant contribution to understand the physicochemical mechanism, several biological and behavioral activities of drugs transported in human body (Kanakis, Tarantilis, Polissiou, Diamantoglou & Tajmir-Riahi 2006; Sarkar, Paul & Mukherjea 2013). HSA is the most abundant protein in blood serum, it accounts for about 60% of the total plasma proteins corresponding to a concentration of 42 mg/mL, and provides about 80% of the colloidal osmotic pressure of blood (Peters Jr 1995). It is the major soluble depot and transport protein, capable of binding, transporting, and delivering an extraordinarily diverse range of endogenous and exogenous compounds like bilirubin, fatty acids, thyroxine, and hemin (Tabachnick 1964; Beaven, D'Albis & Gratzer 1973; Curry, Brick & Franks 1999; Bhattacharya, Grnne & Curry 2000; Zunszain, Ghuman, Komatsu, Tsuchida & Curry 2003; Simard, Zunszain, Hamilton & Curry 2006). HSA also binds to exogenous drug molecules like warfarin, digitoxin, ibuprofen, and quinidine with binding constants of 3.3×10^5, 4×10^5, 2.6×10^6, and 1.6×10^3 M^{-1}, respectively (Varshney et al. 2010). It also maintains normal osmolality in plasma as well as in interstitial fluid and exhibits antioxidant and enzymatic functions (Peters Jr 1995).

HSA has only one tryptophan residue, Trp-214 in the IIA subdomain (Carter et al. 1989; Lakowicz 2006). This protein also contains two principal drug binding sites, Site-I and Site-II. Site-I is located within the hydrophobic cavity of subdomain IIA which is capable of binding mostly neutral, bulky heterocyclic compounds by strong hydrophobic interactions, whereas Site-II is within the IIIA subdomain and binds to many aromatic carboxylic acids by dipole–dipole,

van der Waals and hydrogen bonding interactions (Sudlow, Birkett & Wade 1975; Sudlow, Birkett & Wade 1976; Varshney et al. 2010).

Drug interaction with HSA generally enhances the distribution and bioavailability of the drug depending on the specific pharmacokinetic properties of the drug molecules. Additionally, because of its abundance, HSA play a significant role in the pharmacokinetic behavior of a variety of drugs, including drug half-life in the blood stream, regulating drug efficacy, decreasing drug toxicity and improving drug targeting specificity (Sleep, Cameron & Evans 2013). Therefore, a clear and quantitative information on the nature of a given drug–plasma protein interaction should provide a firm basis for its rational use in clinical practice even if it is not the only factor predictive of serum concentrations of a free drug (Kurono, Fujii, Murata, Fujitani & Negoro 2006; Shang et al. 2014). Recently, we have reported interaction of biologically significant molecules like trimethoxyflavone, asiatic acid, chitosan oligomers, 7-hydroxycoumarin derivatives, piperine, L-dopa and lupeol and its derivatives with HSA (Gokara, Sudhamalla, Amooru & Subramanyam 2010; Gokara, Malavath, Kalangi, Reddana & Subramanyam 2014; Yeggoni et al. 2014; Yeggoni & Subramanyam 2014; Gokara, Kimavath, Podile & Subramanyam 2015; Kallubai, Rachamallu, Yeggoni & Subramanyam 2015; Yeggoni, Rachamallu, Kallubai & Subramanyam 2015).

Nefopam is a centrally acting non-opioid analgesic benzoxazocine and has been used to treat mild to moderate postoperative pain since the mid-1970s (Heel, Brogden, Pakes, Speight & Avery 1980; Kapfer, Alfonsi, Guignard, Sessler & Chauvin 2005; Beloeil, Eurin, Thevenin, Benhamou & Mazoit 2007). In clinical practice, the administration of nefopam has been reported to reduce the use of opioid analgesics, which reduces the prevalence of Postoperative nausea and vomiting (Lee, Kim & Cheong 2013). It is reported that the nefopam plasma half-life is 3-5 h;

with its peak plasma concentrations reaching after 15 – 20 min through intravenous injection. Owing to a first-pass metabolism, oral bioavailability is only 40%. Nefopam undergoes extensive hepatic biotransformation to desmethylnefopam (which seems to be biologically active) and N-oxide-nefopam (Aymard et al. 2003). It is reported that nefopam binding with protein is ~75%, and the major route of elimination (87%) is renal whereas a small part (8%) is excreted in the faeces. Ninety-five per cent of an initial dose is excreted within five days and 5% as unchanged substance (Heel et al. 1980). Nefopam is considered to be safe and well tolerated. Reported adverse effects are mostly minor and includes drowsiness, nausea and vomiting, and sweating (Mimoz et al. 2001; Du Manoir et al. 2003; Kapfer, Alfonsi, Guignard, Sessler & Chauvin 2005). Unlike non-steroidal anti-inflammatory drugs, nefopam has no effect on platelet function and in contrast to opioids, this drug does not seem to increase the risk of respiratory depression (Gasser & Bellville 1975).

In this study, we used synthesized NFs-analogues which are functionalized benzoxazocines (Ramachary, Narayana, Prasad & Ramakumar 2009). Recent studies showed that functionalized benzoxazocines are pharmaceutically acceptable salts that might act as analgesic agents and are used for the treatment of emesis, depression, posttraumatic stress disorders, attention deficit disorders, obsessive compulsive disorders, sexual dysfunction and as centrally acting skeletal muscle relaxants (Stillings et al. 1985; Ohnmacht et al. 2004; Seto, Tanioka, Ikeda & Izawa 2005; Seto, Tanioka, Ikeda & Izawa 2005; Seto, Tanioka, Ikeda & Izawa 2005). Since, nefopam has very important role in pain relief, their products are expensive. It is for this purpose we have attempted to synthesize nefopam analogues which may mimic similar function as original nefopam. To understand the pharmacokinetics with HSA, we have investigated the binding, including quenching mechanisms, binding energies, the number of binding sites, and secondary

structural fluctuations of HSA using spectroscopic methods. Further molecular docking and molecular simulation were also used to gain insight into the binding modes and stability of the NF's-HSA complexes.

2. Materials and Methods

2.1 Synthesis of Nefopam analogues

Nefopam analogues, 1) 6-(phenyl)-7-methyl-9 ethyl 5, 6-dihydro-2H- benzo[b] [1, 4] oxazocine-8-carboxylic acid ethyl ester Nefopam analogue 1 (NF1); 2) 9-(4-chloro phenyl)-6-(4-hydroxy phenyl)-7-methyl-5, 6-dihydro-2H-benzo[b] [1, 4] oxazocine-8-carboxylic acid ethyl ester Nefopam analogue 2 **(NF2)**; 3) 6-(4-hydroxy phenyl)-7-methyl-9-propyl-5, 6-dihydro-2H benzo[b] [1, 4] oxazocine-8-carboxylic acid ethyl ester Nefopam analogue 3 **(NF3)** were synthesised according to our previous method (Ramachary et al. 2009).

General Experimental Procedures for the Synthesis of Nefopam Analogues (NF1, NF2 and NF3) from corresponding Hagemann's esters involves the following three-steps.

Piperidine/K_2CO_3-Catalyzed Three-Component Enamine Amination/Iso-Aromatization/O-Allylation Reactions in One-Pot: In an ordinary glass vial equipped with a magnetic stirring bar, to 1.0 mmol of the Hagemann's esters was added 2.0 mL of solvent, and then the catalyst piperidine (0.05 mmol, 4.95 μL) was added and the reaction mixture was stirred at 25 °C for the 0.5 h; then 0.5 mmol of nitrosobenzene was added in one-portion and the reaction mixture was stirred at 25 °C for 1 h. To the reaction mixture, allyl bromide (181.5 mg, 1.5 mmol) and K_2CO_3 (345.5 mg, 2.5 mmol) were added and stirring continued at RT for 24 h. The crude reaction mixture was worked up with aqueous NH_4Cl solution, and the aqueous layer was extracted with dichloromethane (2 x 20 mL). The combined organic layers were dried (Na_2SO_4), filtered and concentrated. Pure one-pot enamine amination/iso-aromatization/*O*-allylation products were obtained by column chromatography (silica gel, a mixture of hexane/ethyl acetate).

***N*-Allylation:** At 0 °C, to a suspension of sodium hydride (14.4 mg, 0.6 mmol, 3.0 equiv.), in DMF (2 ml, 0.1 M) were added monoene amine (0.2 mmol). After being stirred for 5 min, allyl bromide (48.39 mg, 0.4 mmol, 2.0 equiv.) is added to the reaction mixture at 0 °C, and then the reaction mixture was stirred for 3 to 5 h from 0 °C to RT. The reaction mixture poured into

saturated NH_4Cl solution and extracted with DCM (2 x 15 mL). The combined DCM extracts were washed with brine, dried over Na_2SO_4, and evaporated to dryness. Purification of the residue by column chromatography (silica gel, mixture of hexane/ethyl acetate) gave diene amine product.

RCM Reaction: A 10 ml oven-dried round bottom flask equipped with a stir bar was charged with diene amine (0.1 mmol), CH_2Cl_2 (2 ml, 0.05 M) and first generation Grubb's catalyst (4.11 mg, 0.005 mmol, five mol-%). The reaction mixture was stirred under N_2 at room temperature for 8 to 12 h. Solvent CH_2Cl_2 were distilled off at ambient pressure and the nefopam analogues (NF1, NF2 and NF3) were purified by column chromatography (silica gel, a mixture of hexane/ethyl acetate).

2.2 Sample preparation.

Fat-free HSA (purchased from Sigma-Aldrich) was dissolved in a physiological aqueous solution of 0.1M phosphate buffer pH 7.2 to the final concentration of 1.5mM protein according to the previous procedure (Subramanyam, Gollapudi, Bonigala, Chinnaboina & Amooru 2009). The purity of HSA was confirmed by SDS gel and mass spectrometry (data not shown). The exact concentration of HSA was determined spectrophotometrically using molar extinction coefficient of 35700 M^{-1} cm^{-1} in a Perkin-Elmer lambda 35 (Chatterjee, Pal, Dey, Chatterjee & Chakrabarti 2011). Synthesized NF's were prepared in 20:80 ethanol: distilled water mixture. From our previous work, a solution containing 20% ethanol showed no effect on HSA secondary structure (Subramanyam et al. 2009; Subramanyam et al. 2009). The optimum physiological pH for HSA was set to be 7.2 as it has the maximum absorption and fluorescence at this pH (Subramanyam et al. 2009; Subramanyam et al. 2009). Thus, for all the experiments, we have used 0.1 M phosphate buffer at pH 7.2 as a physiological buffer. The optimum incubation time for binding of NF1, NF2, and NF3 with HSA was found to be 15 min as assessed by fluorescence emission spectroscopy. Thus, we followed the same incubation time for all the experiments.

2.3 Fluorescence spectroscopy studies.

A quantitative analysis of the potential interaction between NF1, NF2, and NF3 with HSA was performed by LS-55 Spectrofluorimeter (PerkinElmer, USA), with 1.0 cm quartz cells. Fluorescence emission spectra were recorded at 25 ^{O}C with a wavelength range of 300–450 nm and excited at 285nm. The bandwidth was fixed to 5.0 nm for both excitation and emission. The sample temperature was maintained at 25 ^{O}C. HSA concentration was $1x10^{-6}$M, and the concentrations of NFs were 1 to 9μM in 0.1M phosphate buffer with pH 7.2 (physiological pH). Three independent experiments were performed and each time identical spectra were obtained. All protein fluorescence spectra were corrected by subtraction of buffer. Furthermore, the spectra were corrected to avoid inner filter effect by using the below equation.

The intensity of fluorescence observed (F_{obs}) was corrected for inner filter effect (F_{or}) (Kirby 1971; Lakowicz 2006)

$$\mathrm{Fcor} = \mathrm{Fobs}10\ (\mathrm{A}exc + \mathrm{A}emi)/2 \quad [1]$$

Where, F_{or} is the corrected fluorescence intensity, A_{exc} and A_{emi} represent the absorbance at the fluorescence excitation (285 nm) and emission wavelengths (360 nm) for HSA and (340 nm) for AGP. Fobs are the observed fluorescence (Lakowicz 2006). The corrected values allow evaluating fluorescence quenching only due to the interaction of the drug with albumin (van de Weert & Stella 2011). The detailed procedure was given in our previously published articles and also can be referred these articles for further details (Subramanyam et al. 2009; Subramanyam et al. 2009; Gokara et al. 2015).

2.4 Displacement experiments with Site I (Phenylbutazone) and II (Ibuprofen) and lidocaine Markers.

For the competitive phenylbutazone/ibuprofen/Lidocaine HSA experiment, the concentrations of HSA and the site probe were maintained at a constant concentration of 1 μM, whereas nefopam analogues were titrated with increasing concentrations of NF-1, 2, and three from 1 μM -9 μM. The excitation wavelength for phenylbutazone, ibuprofen and Lidocaine complexes with HSA was 285 nm (Yeggoni et al. 2014).

2.5 Circular Dichroism

Circular dichroism (CD) measurements were made on a Jasco J-810 spectropolarimeter (JAPAN) using a quartz cell with a path length of 0.2 cm cell in a nitrogen atmosphere. The spectra were recorded in the range of 190 to 300 nm, and the scan rate is 50 nm/min with a response time of 4 s. All the parameters were followed according to our previous procedures (Subramanyam et al. 2009; Subramanyam et al. 2009). The induced ellipticity of the protein alone was defined as the ellipticity of the drug-HSA mixture minus the ellipticity of drug alone at the same wavelength. The concentration of HSA was 0.001mM ($1x10^{-6}$M) and the concentrations of NF1, NF2 and NF3 were 0.001, 0.005, and 0.009mM, respectively. Each time three scans were averaged and likewise three independent spectra were measured with identical spectra. The relative contents of secondary structure; α-helix, β-pleated sheet, β-turn, and random coils of HSA were calculated by using CDNN 2.1 software S Table 1). All the Spectra were corrected for baseline with respective blanks for HSA control and NF's-HSA complexes.

2.6 Molecular docking

Since the experimental evidence showed NF's binding to HSA, we were interested in pinpointing the probable binding mechanism and important interactions in atomic details in the binding site via molecular docking. AutoDock program (Version AutoDock 4.2.3) was used to identify the

potential ligand binding sites (Morris et al. 2009). Lamarckian genetic algorithm (LGA) implemented in AutoDock was applied to estimate the possible conformations of the ligand–protein complex. HSA crystal structure used in the docking studies was obtained from the RCSB Protein Data Bank (PDB ID: 1AO6). The receptor (HSA) and NF'S were pretreated. For the ligand preparation, 3D structures of NF1, NF2, and NF3 were built from their 2D structures, and their geometry was optimized using discovery studio 3.5 software according to our previous work (Yeggoni et al. 2014; Gokara et al. 2015). For the recognition of all binding sites in HSA, docking was performed by setting the grid box size at 126 Å 126 Å 126 Å, which was followed by blind docking (Hetenyi & van der Spoel 2006). All the parameters were inserted at their default settings. Among 30 conformations, the conformer with the lowest binding free energy was also matched with experimental data for further analysis as reported earlier (Sudhamalla, Gokara, Ahalawat, Amooru & Subramanyam 2010; Malleda, Ahalawat, Gokara & Subramanyam 2012). Further to elucidate the affinity of nefopham analogues over other analogues we have carried out docking with nefopham-aliphatic (NF-R1), Nefopham-bromide (NF-R2), nefopham-cholride (NF-R3) (for structures see Figure S2.). These three analogues where docked with the three binding sites i.e., IB, IIA and IIIA. The result with the lowest docking energy analysis in cluster rank 1 was used for further analysis. For visualization of the docked conformations, Pymol v 1.5 was used. All the parameters that are mentioned above were according to our previous work (Sudhamalla et al. 2010; Yeggoni et al. 2014; Gokara et al. 2015).

2.7 Molecular dynamic simulations (MD Simulation)

The structure of NF's-HSA complexes obtained from the docking procedure was used as starting point for the MD simulation. A 10 ns MD simulation was carried out using GROMOS96 force-

field through the GROMACS4 software (Ver. 4.5, www.gromacs.org) (Berendsen, van der Spoel & van Drunen 1995; van Gunsteren et al. 1996; Van Gunsteren, Daura & Mark 1998). The topology parameters of HSA were created by using Gromacs program. The topology parameters of NF1, NF2, and NF3 were built by the Dundee PRODRG2.5 server (Schuttelkopf & van Aalten 2004). Then the complex was immersed in a cubic box (7.335×6.135×8.119nm) of extended simple point charge water molecules (Berendsen, Postma, Van Gunsteren & Hermans 1981). All the parameters that are mentioned above were according to our previous work (Sudhamalla et al. 2010; Yeggoni et al. 2014; Gokara et al. 2015). The MD simulation and results analysis were performed on OSCAR Linux cluster with 16 nodes (dual xeon processor) at Bioinformatics Facility, School of Life Sciences, and University of Hyderabad.

3. Results and discussion

To study the binding mechanism of Nefopam analogous with HSA, the fluorescence emission spectra is an important tool shown in Figure 1. When the excitation wavelength is set at 285 nm, HSA shows a strong emission band around 360 nm. The continuous addition of NFs, the fluorescence maxima of HSA decreased gradually, which reveals NF's quenched the intrinsic fluorescence of HSA. Dynamic and static quenching mainly causes fluorescence quenching. Thus, dynamic and static quenching can be distinguished by temperature and viscosity, or by the difference in their fluorescence lifetime (Lakowicz 2006). Dynamic quenching is a process in which the fluorophore and the quencher come into contact during the transient existence of the excited state. Static quenching refers to fluorophore (HSA)-quencher (NF's) complex formation. To verify whether the quenching is static or dynamic in NF-HSA complexes, bimolecular quenching constant were calculated from the slope of F_0/F vs. [Q] (S-Figure 1), which are found

to be linear for NFs- HSA complexes indicating that the quenching is mainly static. The Kq was estimated according to the Stern-Volmer equation:

$$\frac{Fo}{F} = 1 + k_q t_0[Q] = 1 + K_D[Q] \qquad [2]$$

Where F_O and F are the fluorescence intensities in the absence and presence of quencher, [Q] is the quencher concentration, and K_D is the Stern-Volmer quenching constant (K_q), which can be written as $K_D=k_qt_0$; where k_q is the bimolecular quenching rate constant, and t_0 is the lifetime of the fluorophore in the absence of quencher, lifetime of fluorophore for HSA been 5.6 ns (Tayeh, Rungassamy & Albani 2009).

The rate constant (Kq) of NF1, NF2 and NF3 were 5.5×10^{13}, 5.4×10^{13} and 4×10^{13} M^{-1} S^{-1}, respectively. In general, the collisional quenching constant for various types of quencher with biopolymer is 2.0×10^{10} L/mol/s (Zhang, Que, Pan & Guo 2008). From the analysis, it is apparent that bimolecular quenching constants are much greater than this value, which implies that there is non-fluorescent complex formation between the NFs and HSA. The static quenching may be the main mechanism of the fluorescence quenching of HSA by NFs under our experiment conditions.

For static quenching, the binding constant (Ks) and the number of binding sites (n) can be obtained from modified Stern–Volmer regression curves based on the following equation (Zsila, Bikádi & Simonyi 2003; Min et al. 2004).

$$\log\left[\left(F_0 - F\right) \div F\right] = \log K_s + n \times \log[Q] \qquad [3]$$

Where n is the slope (i.e. the number of binding sites), K_s is the binding constant and [Q] is the quencher concentration. The results showed that the number of Nefopam molecules binding

to HSA was about 0.87, 0.96 and 0.9 for NF1, NF2 and NF3 respectively, which indicates that the binding of NFs was approximately one to one ratio for HSA (Figure 1, inserts). From the intercept of the plot, the binding constants of NF1, NF2 and NF3 with HSA was calculated from the intercept as $1.53 \pm 0.057 \times 10^4$, $2.16 \pm 0.071 \times 10^4$ and $3.6 \pm 0.102 \times 10^5$ M^{-1} for NF1, NF2 and NF3, respectively (Figure 1), which indicates strong binding of these analogues with HSA. The order of the binding constants for these analogues are NF3>NF2>NF1. The different binding constants between these three analogues are due to the variation in the functional groups. This is concurrence with our recent report which was synthesized molecules of different coumarin derivatives with the various functional group attached behaved the similar kind of binding (Archit et al. 2013; Yeggoni et al. 2014). Further, we have discussed about the role of functional groups in docking results.

Site-specific marker analysis of HSA with Nefopam analogues.

Displacement experiments were employed with constant one μM concentration of HSA and for the site-specific probes. The intensity of the HSA-site probe fluorescence was recorded with the increasing concentrations of NF's. Remarkably, fluorescence quenching of NF'-HSA complexes was observed with titration of different concentrations of NF-1, NF-2, and NF-3 with respective site markers, i.e., Ibuprofen, lidocaine, and phenylbutazone. The binding constant values obtained for NF's with HSA were found to be more than the HSA-site markers, which indicates that there is competition between NF's and site-specific markers (Table 1). Additionally, to make sure that whether the NF's have more than one binding site, we performed fluorescence with site markers in different combinations; which showed insignificant fluorescence quenching/no fluorescence quenching. With this experimental evidence, we can firmly assure that three NF's have only one specific binding site.

3.1 Free energy calculations

Fundamentally, there are four main types of non-covalent interactions involves the interactions of ligands with proteins, including hydrogen bonding, van der Waals forces, hydrophobic and electrostatic interactions (Qi et al. 2008). The signs and magnitudes of the thermodynamic parameters for protein reactions can be accounted to identify the main forces contributing to ligand–protein stability. Free energy can depict the type of interactions involved in the formation of NF1, NF2 and NF3 and HSA-Nfs complexes. The free energy (ΔG^0) of the binding was calculated from the following equation:

$$\Delta G^\circ = -RT \ln K \qquad [4]$$

Where, ΔG is free energy, K is the binding constant at the corresponding temperature, which can be obtained from fluorescence data, R is the gas constant and T is absolute temperature.

The standard free energies were calculated to be approximately -5.48, -5.7 and -7.50 kcal/mol for NF1, NF2 and NF3 respectively at 25 ^{o}C. These results indicate that HSA-NF3 complex is more stable than the HSA-NF2 and HSA-NF1. Docking experiments revealed that the mode of binding between NF1, NF2 and NF3 and HSA were located in three different domains. Even though the backbone of these NFs is the same but the variation in the binding is due to the differences in the functional groups. The small change in the functional group would obvious change of the acceptability of the drug and their binding. Our recent studies showed such kind of interactions played an important role in the binding of biologically significant drugs in the formation of HSA-Drug complexes (Gokara et al. 2014; Yeggoni et al. 2014; Gokara et al. 2015; Yeggoni et al. 2015).

3.2 Secondary Structure analysis: Studied by Circular Dichroism

To decipher the secondary structural changes of HSA caused by its interaction with NF's, we have carried out CD experiment of HSA in the presence of different concentrations of NF's. CD spectroscopy is one of the best tools to monitor the structure, conformation, and stability of proteins in solution. It can provide us with a very good estimation of the fraction of the residues in the protein structures which are involved in α -helical, β -sheet, turn, and random coil and possibly their inter-conversions. The CD spectrum of native HSA in far-UV region has two negative bands in the region of 208 and 222 nm (Li et al. 2005; Yeggoni et al. 2014), which is characteristic of α-helix. When various concentrations of NF1, NF2 and NF3 were added to free HSA the intensity at 208 and 222 nm decreased in a concentration-dependent manner (Figure 2). The decrease of α-helix, increasing order of β-helix and random coils follows as NF3>NF2>NF1 (Figure 2, Figure 3 and S Table 1). Conformational analysis revealed that α-helix of HSA while binding with three analogues were decreased, while consequent increase (in %) in the β-sheets and random coils, NF1: α-helix; 57.2±2.5 to 47±2.5: β-sheets; 25±0.8 to 30.8±1: Random Coil; 17.8±1.0 to 22.2±1.2. NF2: α-helix; 57.2±2.5 to 41.7±1.82: β-sheets; 25±0.9 to 32.4±1.02: Random coil; 17.9±1.8 to 25.9±2.6.NF3: α-helix; 57.1±2.5 to 36.8±1.6: β-sheets; 25±0.88 to 34.1±1.07: Random coil; 17.9±1.82 to 29.1±2.94. The decrease in the α-helix accompanied with the increase in the β-sheets and random coils indicated the partial unfolding of HSA with NFs analogues, suggesting the formation of NFs-HSA complexes. The difference in the conformational changes of NF's is attributed to their structural complexity, which is in the order of NF3>NF2>NF1 and this might be the reason for alteration of protein conformation. This is very well supported by fluorescence studies where the order of binding affinity is (NF3>NF2>NF1) suggesting that with an increase in binding affinity leads to the decrease in the

secondary structure of the protein. The differences in α-helical contents can be attributed to the different structural arrangements of the protein in solid state and in aqueous solution. Similar conformational transitions from α-helix to β-sheet structure were observed for protein unfolding (Li et al. 2005). Thus, upon binding of NFs to HSA, the secondary structure appears to be partially unfolded due to change in microenvironment of the protein. Similar studies were reported by our group that upon binding of different drug molecules to HSA lead to the change in protein conformation (Sudhamalla et al. 2010; Yeggoni et al. 2014; Gokara et al. 2015; Yeggoni et al. 2015).

3.3 Molecular Docking Studies

Molecular docking was employed to understand the interaction NF's with specific binding sites on HSA. The binding location of NF's with HSA molecule is of crucial importance. Since the knowledge of the binding location within the protein environment of a biologically active drug molecule is a crucial prerequisite for understanding the efficacy and also its function as a therapeutic agent. The docking results indicated that among the NF's, NF1 is bound to the Sudlow site 2 i.e., IIIA (Figure 4A, 4B and 4C) surrounded by Val 409, Arg 410, Thr 540, Leu 544, Glu 542, Leu 529, Lys 545, Ala 406, Asn 405; NF2 is bound to IB (Figure 4D, 4E and 4F) Met 125, Pro 118, Arg 117, Val 116, Phe 134, Leu 182, Leu 115, Tyr 161, Lys 137, Tyr 138, Glu 141, Ile 142, His 146 and NF3 is bound to Sudlow site 1, i.e., IIA (Figure 4G, 4H and 4I) Glu 208, Arg 209, Lys 212, Ala 213, Val 216, Asp 324, Val 325, Phe 228, Leu 327, Gly 328, Glu 354, Leu 331, Ala 350. It is observed that among the three analogues only NF1 has two hydrogen bonds (Figure 4B) with Lys 413 with the bond length of 2.1 Å and 2.6 Å, whereas NF2 and NF3 are stabilized completely by hydrophobic interactions (Figure 4E and Figure 4H). Furthermore,

the binding of NF2 with non-conventional site, i.e., Subdomain IB might lead to the exposure of hydrophobic cavity of Subdomain IIA, which is in perfect agreement with the fluorescence of NF2-HSA, which showed the red shift of NF2-HSA fluorescence. Although there are no studies reported with nefopam, there are other studies which showed that non-opioid analgesics like phenylbutazone, indomethacin bind strongly with HSA with binding constants of 7.0×10^5 and 1.4×10^6 M^{-1}, respectively (Varshney et al. 2010). The calculated binding energies of NF1, NF2, and NF3 are -5.66, -5.90, -7.57 Kcal M^{-1}, respectively. These values are close and corroborate with the experimental values suggesting that these analogues are strong enough to bind with HSA, which is important for proper disposition and therapeutic action.

For further validation to understand the functional group role in binding, we performed docking with HSA to NF-R1$(CH_2)_5$, NF-R2 (Br) and NF-R3 (Cl). The analysis of docking results (See S Table 2) showed that nefopham analogues are having higher affinity and free energies compared with NF-R1, NF-R2 and NF-R3. Despite of binding within the same proximity, NF with different R groups showed less binding, which clearly suggests that functional groups of NF1, NF2 and NF3 plays a central role in forming stable complexes with HSA with more binding and free energies. Thus, other than NFs analogous the additionally added R groups like NF-R1$(CH_2)_5$, NF-R2 (Br) and NF-R3 (Cl) are binding with different amino acids in same binding pocket (See Figure S2 to 5). Hence, the docking results of NF-R1$(CH_2)_5$, NF-R2 (Br) and NF-R3 (Cl) are having weaker binding when compare to the proposed NFs analogous, suggested that NFs analogues have good binding activity.

3.4 Molecular dynamics simulations

The NF's-HSA complexes were further analyzed by MD simulations to evaluate the reliability of the docking results and the stability of the complexes. Complexes of NF analogues and HSA were simulated for ten ns using the GROMACS MD package as discussed in materials and methods.

The root mean square deviation (RMSD) of the trajectories from their initial structures was used to examine whether the structure of the NFs- HSA complex remained stable or not under the simulation conditions (Figure 5). As seen in Figure 5 during the MD simulations the RMSD reached a plateau after the first 2.5 ns. After that the deviations in RMSD (nm) are nearly equal for HSA alone and NFs-HSA complexes, with a subsequent increase up to the start of the Cα-backbone of the HSA, and NFs-HSA analogues are stabilized at approximately 2.5 ns. Further, it remained stable without any drastic fluctuations till the end of the simulation indicating that the molecular system well behaved after that. Interestingly the fluctuations of RMSD are in perfect agreement with the CD data. Order of fluctuations with respect to Cα-backbone of HSA are in the order of NF2>NF3>NF1, compared to CD studies as it is in the order of NF3>NF2>NF1. The difference might be due to the binding of NF2 in the different domain, i.e., IB; it is believed that the drugs bind to subdomain IIA and IIIA. However, recently it was reported that IB is also involved in the binding (Zsila 2013). The possible explanation can be drawn from the fluorescence graph (see Figure 1B), where there is a red shift in the emission maximum of NF2-HSA complexes. Indicating that binding of NF2 induced conformational changes globally (i.e., Cα-backbone) but not strong enough to induce a conformational change in secondary structural elements (α-helix, β-sheets, and random coils). This is in perfect agreement with Rg data (Figure. 6B).

Rg gives the compactness/structural integrity of the HSA values against time, and it describes the overall spread of the molecule (HSA). It is defined as the root-mean-square distance of the collection of atoms from their common center of gravity. In the present MD studies, we determined the Rg values of free HSA and NFs-HSA complexes as shown in Figure 6, in which it is observed that the compactness of NF1-HSA is almost the same as HSA. Whereas with NF2-HSA and NF3-HSA the peaks at around 4.5 – 6.5 ns are deviated about 1.5 ± 0.25 Å with respect to HSA.

To evaluate the NF's binding site and its reliability with HSA, we analyzed root mean square fluctuation (RMSF). These studies indicated that IIIA, IB, and IIA are rigid with respect to the remaining domains of NFs-HSA complexes (Figure 7). This is consistent with docking studies suggesting that NF1, NF2, and NF3 specifically bind with IIIA, IB and IIA, respectively.
As mentioned earlier that the differential binding could be various functional molecules present in the NF's. These MD simulations support that the HSA binding sites IIIA, IB and IIA specifically interact with NFs through conformational changes which allow to modify several molecular properties of HSA at different times (ns) or even at the same time without any significant loss of local conformations of HSA. Previously we have reported similar kind of work which showed MD simulations are consistent with the experimental data (Sudhamalla et al. 2010; Malleda et al. 2012; Gokara et al. 2014; Yeggoni et al. 2014; Gokara et al. 2015). Furthermore, this supports the notion that the HSA protein is ligand promiscuous, as it shows several binding sites at different time points within movements that conserve its 3D structure.

4. Conclusion

In conclusion, interaction and secondary structural changes of HSA with NF-analogues were analyzed using fluorescence and CD spectroscopy, molecular docking and molecular dynamics

techniques. The results revealed that NF-analogues quenched HSA fluorescence via static quenching. The affinity of NF analogues–HSA was diverse for three analogues which are in the descending order as NF3>NF2>NF1. The negative values of ΔG indicated that the binding processes were spontaneous; hydrophobic interactions were considered to be the main binding force between NF analogues and HSA except NF1, which has one hydrogen bond. Conformational analysis revealed that α-helix of HSA with three analogues decreased with consequent increase in the β-sheets and random coils. The structural perturbation of HSA indicates NF's complexation has minimal effect on the secondary structure of HSA which is further supported by molecular simulations, from which it can be presumed that the inherent function of HSA wasn't affected. Binding site analysis by docking study validated that among NF analogues NF1, NF2 and NF3 bound to IIIA, IB, and IIA binding sites respectively. Molecular simulations studies revealed that RMSD fluctuations remained the same after 2.5 ns without any fluctuations for three analogues, whereas Rg indicated that compactness of NF1-HSA is almost the same as HSA, whereas with NF2-HSA and NF3-HSA the peaks at around 4.5 – 6.5 ns deviate about 1.5 ± 0.25 Å with respect to HSA. RMSF indicated that NF1, NF2, and NF3 are specifically binding with IIIA, IB and IIA, respectively which reflects that the compactness of HSA remains rigid after the binding. Hence, the interaction between HSA and NF-analogues will be an important factor in our understanding of the pharmacokinetics and pharmacological effects of NF analogues.

ACKNOWLEDGMENTS

We thank CIL, and BIF for CD and computational facility, University of Hyderabad, India. We thank UPE-I and II, UGC, UGC-DSKPDF India for financial support. We dedicate this article for our coauthor Mr. Chandramouli Malleda who passed away during the preparation of this manuscript.

References

Ahmad, B., Parveen, S. & Khan, R. H. (2006). Effect of albumin conformation on the binding of ciprofloxacin to human serum albumin: a novel approach directly assigning binding site. Biomacromolecules 7: 1350-1356.doi:dx.doi.org/10.1021/bm050996b

Archit, G., Mark Manidhar, D., Mahesh, G., Chandramouli, M., Suresh Reddy, C. & Rajagopal, S. (2013). Elucidation of the Binding Mechanism of Coumarin Derivatives with Human Serum Albumin. PLoS One 28. doi:10.1371/journal.pone.0063805

Aymard, G., Warot, D., Demolis, P., Giudicelli, J. F., Lechat, P., Le Guern, M. E., Alquier, C. Diquet, B. (2003). Comparative pharmacokinetics and pharmacodynamics of intravenous and oral nefopam in healthy volunteers. Pharmacol Toxicol 92: 279-286. doi:dx.doi.org/10.1034/j.1600-0773.2003.920605.x

Beaven, G. H., D'Albis, A. & Gratzer, W. B. (1973). The interaction of bilirubin with human serum albumin. European Journal of Biochemistry 33: 500-509.doi: dx.doi.org/10.1111/j.1432-1033.1973.tb02709.x

Beloeil, H., Eurin, M., Thevenin, A., Benhamou, D. & Mazoit, J. X. (2007). Effective dose of nefopam in 80% of patients (ED80): a study using the continual reassessment method. Br J Clin Pharmacol 64: 686-693.doi:dx.doi.org/10.1111/j.0306-5251.2007.02960.x

Berendsen, H., Postma, J., Van Gunsteren, W. & Hermans, J. (1981). Interaction models for water in relation to protein hydration. Intermolecular forces 11(1): 331-342.doi: 10.1007/978-94-015-7658-1_21

Berendsen, H. J., van der Spoel, D. & van Drunen, R. (1995). GROMACS: A message-passing parallel molecular dynamics implementation. Computer Physics Communications 91: 43-56.doi:dx.doi.org/10.1016/0010-4655(95)00042-E

Bhattacharya, A. A., Grnne, T. & Curry, S. (2000). Crystallographic analysis reveals common modes of binding of medium and long-chain fatty acids to human serum albumin. Journal of Molecular Biology 303: 721-732.doi:dx.doi.org/10.1006/jmbi.2000.4158

Carter, D. C., He, X.-M., Munson, S. H., Twigg, P. D., Gernert, K. M., Broom, M. B. & Miller, T. Y. (1989). Three-dimensional structure of human serum albumin. Science 244: 1195-1198. doi:dx.doi.org/10.1126/science.2727704

Carter, D. C. & Ho, J. X. (1994). Structure of serum albumin. Advances in Protein Chemistry 45: 153-203.doi:dx.doi.org/10.1016/S0065-3233(08)60640-3

Chatterjee, T., Pal, A., Dey, S., Chatterjee, B. & Chakrabarti, P. (2011). Interaction of virstatin with human serum albumin: spectroscopic analysis and molecular modeling. PLoS One 7: e37468-e37468.doi:dx.doi.org/10.1371/journal.pone.0037468

Curry, S., Brick, P. & Franks, N. P. (1999). Fatty acid binding to human serum albumin: new insights from crystallographic studies. Biochimica et Biophysica Acta 1441: 131-140. doi:dx.doi.org/10.1016/S1388-1981(99)00148-1

Du Manoir, B., Aubrun, F., Langlois, M., Le Guern, M. E., Alquier, C., Chauvin, M. & Fletcher, D. (2003). Randomized prospective study of the analgesic effect of nefopam after orthopaedic surgery. Br J Anaesth 91: 836-841.doi:dx.doi.org/10.1093/bja/aeg264

Gasser, J. & Bellville, J. (1975). Respiratory effects of nefopam. Clinical pharmacology and therapeutics 18: 175-179.doi:dx.doi.org/10.1002/cpt1975182175

Gokara, M., Kimavath, G. B., Podile, A. R. & Subramanyam, R. (2015). Differential nteractions and structural stability of chitosan oligomers with human serum albumin and alpha-1-glycoprotein. Journal of Biomolecular Structure and Dynamics 33: 196-210. doi:dx.doi.org/10.1080/07391102.2013.868321

Gokara, M., Malavath, T., Kalangi, S. K., Reddana, P. & Subramanyam, R. (2014). Unraveling the binding mechanism of asiatic acid with human serum albumin and its biological implications. Journal of Biomolecular Structure and Dynamics 32: 1290-1302. doi:dx.doi.org/10.1080/07391102.2013.817953

Gokara, M., Sudhamalla, B., Amooru, D. G. & Subramanyam, R. (2010). Molecular interaction studies of trimethoxy flavone with human serum albumin. PLoS One 5: e8834. doi:dx.doi.org/10.1371/journal.pone.0008834

Heel, R. C., Brogden, R. N., Pakes, G. E., Speight, T. M. & Avery, G. S. (1980). Nefopam: a review of its pharmacological properties and therapeutic efficacy. Drugs 19: 249-267. doi:dx.doi.org/10.2165/00003495-198019040-00001

Hetenyi, C. & van der Spoel, D. (2006). Blind docking of drug-sized compounds to proteins with up to a thousand residues. FEBS Letters 580: 1447-1450. doi:dx.doi.org/10.1016/j.febslet.2006.01.074

Kallubai, M., Rachamallu, A., Yeggoni, D. P. & Subramanyam, R. (2015). Comparative binding mechanism of lupeol compounds with plasma proteins and its pharmacological importance. Mol Biosyst 11: 1172-1183.doi:dx.doi.org/10.1039/C4MB00635F

Kanakis, C. D., Tarantilis, P. A., Polissiou, M. G., Diamantoglou, S. & Tajmir-Riahi, H. A. (2006). Antioxidant flavonoids bind human serum albumin. Journal of Molecular Structure 798: 69-74.doi:dx.doi.org/10.1016/j.molstruc.2006.03.051

Kapfer, B., Alfonsi, P., Guignard, B., Sessler, D. I. & Chauvin, M. (2005). Nefopam and ketamine comparably enhance postoperative analgesia. Anesth Analg 100: 169-174.doi:dx.doi.org/10.1213/01.ANE.0000138037.19757.ED

Kapfer, B., Alfonsi, P., Guignard, B., Sessler, D. I. & Chauvin, M. (2005). Nefopam and Ketamine Comparably Enhance Postoperative Analgesia. Anesthesia and analgesia 100: 169-174.doi:dx.doi.org/10.1213/01.ANE.0000138037.19757.ED

Kirby, E. (1971). Fluorescence Instrumentation and Methodology. Excited States of Proteins and Nucleic Acids. R. Steiner and I. Weinryb, Springer US: 31-56.doi:dx.doi.org/10.1007/978-1-4684-1878-1_2

Kurono, M., Fujii, A., Murata, M., Fujitani, B. & Negoro, T. (2006). Stereospecific recognition of a spirosuccinimide type aldose reductase inhibitor (AS-3201) by plasma proteins: A significant role of specific binding by serum albumin in the improved potency and stability. Biochemical Pharmacology 71: 338-353.doi:dx.doi.org/10.1016/j.bcp.2005.10.036

Lakowicz, J. R. (2006). Principles of Fluorescence Spectroscopy. Principles of Fluorescence Spectroscopy, by JR Lakowicz. ISBN 0-387-31278-1. Berlin: Springer, 2006. 1.doi:dx.doi.org/10.1007/978-0-387-46312-4

Lee, J. H., Kim, J. H. & Cheong, Y. K. (2013). The Analgesic Effect of Nefopam with Fentanyl at the End of Laparoscopic Cholecystectomy. The Korean Journal of Pain 26: 361-367.doi:dx.doi.org/10.3344/kjp.2013.26.4.361

Li, Y., He, W., Liu, J., Sheng, F., Hu, Z. & Chen, X. (2005). Binding of the bioactive component Jatrorrhizine to human serum albumin. Biochimica et Biophysica Acta (BBA) - General Subjects 1722: 15-21.doi:dx.doi.org/10.1016/j.bbagen.2004.11.006

Malleda, C., Ahalawat, N., Gokara, M. & Subramanyam, R. (2012). Molecular dynamics simulation studies of betulinic acid with human serum albumin. Journal of Molecular Modeling 18: 2589-2597.doi:dx.doi.org/10.1007/s00894-011-1287-x

McLintock, T. T., Kenny, G. N., Howie, J. C., McArdle, C. S., Lawrie, S. & Aitken, H. (1988). Assessment of the analgesic efficacy of nefopam hydrochloride after upper abdominal surgery: a study using patient controlled analgesia. Br J Surg 75: 779-781.doi:dx.doi.org/10.1002/bjs.1800750818

Mimoz, O., Incagnoli, P., Josse, C., Gillon, M. C., Kuhlman, L., Mirand, A., Soilleux, H. & Fletcher, D. (2001). Analgesic efficacy and safety of nefopam vs. propacetamol following hepatic resection. Anaesthesia 56: 520-525.doi:dx.doi.org/10.1046/j.1365-2044.2001.01980.x

Min, J., Meng-Xia, X., Dong, Z., Yuan, L., Xiao-Yu, L. & Xing, C. (2004). Spectroscopic studies on the interaction of cinnamic acid and its hydroxyl derivatives with human serum albumin. Journal of Molecular Structure 692: 71-80. doi:dx.doi.org/10.1016/j.molstruc.2004.01.003

Morris, G. M., Huey, R., Lindstrom, W., Sanner, M. F., Belew, R. K., Goodsell, D. S. & Olson, A. J. (2009). AutoDock4 and AutoDockTools4: Automated docking with selective receptor flexibility. Journal of Computational Chemistry 30: 2785-2791.doi:dx.doi.org/10.1002/jcc.21256

Ohnmacht, C. J., Albert, J. S., Bernstein, P. R., Rumsey, W. L., Masek, B. B., Dembofsky, B. T., Koether, G. M., Andisik, D. W. & Aharony, D. (2004). Naphtho[2,1-b][1,5] and [1,2-f][1,4]oxazocines as selective NK1 antagonists. Bioorganic & Medicinal Chemistry 12: 2653-2669.doi:dx.doi.org/10.1016/j.bmc.2004.03.015

Peters Jr, T. (1995). All about Albumin: Biochemistry, Genetics and Medical Applications. San Diego, CA: Academic Press. Retrived from http://library.wur.nl/WebQuery/clc/1864656

Qi, Z.-d., Zhang, Y., Liao, F.-l., Ou-Yang, Y.-w., Liu, Y. & Yang, X. (2008). Probing the binding of morin to human serum albumin by optical spectroscopy. Journal of Pharmaceutical and Biomedical Analysis 46: 699-706.doi:dx.doi.org/10.1016/j.jpba.2007.10.016

Ramachary, D. B., Narayana, V. V., Prasad, M. S. & Ramakumar, K. (2009). High-yielding synthesis of Nefopam analogues (functionalized benzoxazocines) by sequential one-pot cascade operations. Org Biomol Chem 7: 3372-3378.doi:dx.doi.org/10.1039/b910397j

Sarkar, M., Paul, S. S. & Mukherjea, K. K. (2013). Interaction of bovine serum albumin with a psychotropic drug alprazolam: Physicochemical, photophysical and molecular docking studies. Journal of Luminescence 142: 220-230.doi:dx.doi.org/10.1016/j.jlumin.2013.03.026

Schuttelkopf, A. W. & van Aalten, D. M. (2004). PRODRG: a tool for high-throughput crystallography of protein-ligand complexes. Acta Crystallographica Section D: Biological Crystallography 60: 1355-1363.doi:dx.doi.org/10.1107/S0907444904011679

Seto, S., Tanioka, A., Ikeda, M. & Izawa, S. (2005). 2-Substituted-4-aryl-6,7,8,9-tetrahydro-5H-pyrimido[4,5-b][1,5]oxazocin-5-one as a structurally new NK1 antagonist. Bioorganic & Medicinal Chemistry Letters 15: 1485-1488.doi:dx.doi.org/10.1016/j.bmcl.2004.12.089

Seto, S., Tanioka, A., Ikeda, M. & Izawa, S. (2005). Design and synthesis of novel 9-substituted-7-aryl-3,4,5,6-tetrahydro-2H-pyrido[4,3-b]- and [2,3-b]-1,5-oxazocin-6-ones as NK1 antagonists. Bioorganic & Medicinal Chemistry Letters 15: 1479-1484. doi:dx.doi.org/10.1016/j.bmcl.2004.12.091

Seto, S., Tanioka, A., Ikeda, M. & Izawa, S. (2005). Design, synthesis, and evaluation of novel 2-substituted-4-aryl-6,7,8,9-tetrahydro-5H-pyrimido[4,5-b][1,5]oxazocin-5-ones as NK1 antagonists. Bioorganic & Medicinal Chemistry 13: 5717-5732. doi:dx.doi.org/10.1016/j.bmc.2005.06.015

Shang, S., Liu, Q., Gao, J., Zhu, Y., Liu, J., Wang, K., Shao, W. & Zhang, S. (2014). Insights into In Vitro Binding of Parecoxib to Human Serum Albumin by Spectroscopic Methods. Journal of Biochemical and Molecular Toxicology 28: 433-441.doi:dx.doi.org/10.1002/jbt.21582

Simard, J. R., Zunszain, P. A., Hamilton, J. A. & Curry, S. (2006). Location of high and low affinity fatty acid binding sites on human serum albumin revealed by NMR drug-competition analysis. Journal of Molecular Biology 361: 336-351.doi:dx.doi.org/10.1016/j.jmb.2006.06.028

Sleep, D., Cameron, J. & Evans, L. R. (2013). Albumin as a versatile platform for drug half-life extension. Biochimica et Biophysica Acta (BBA) - General Subjects 1830: 5526-5534. doi:dx.doi.org/10.1016/j.bbagen.2013.04.023

Stillings, M. R., Freeman, S., Myers, P. L., Readhead, M. J., Welbourn, A. P., Rance, M. J. & Atkinson, D. C. (1985). Substituted 5H-dibenz[b,g]-1,4-oxazocines and related amino acids with antiinflammatory activity. Journal of Medicinal Chemistry 28: 225-233. doi:dx.doi.org/10.1021/jm00380a013

Subramanyam, R., Gollapudi, A., Bonigala, P., Chinnaboina, M. & Amooru, D. G. (2009). Betulinic acid binding to human serum albumin: A study of protein conformation and binding affinity. Journal of Photochemistry and Photobiology B: Biology 94: 8-12. doi:dx.doi.org/10.1016/j.jphotobiol.2008.09.002

Subramanyam, R., Goud, M., Sudhamalla, B., Reddeem, E., Gollapudi, A., Nellaepalli, S., Yadavalli, V., Chinnaboina, M. & Amooru, D. G. (2009). Novel binding studies of human serum albumin with trans-feruloyl maslinic acid. Journal of Photochemistry and Photobiology B: Biology 95: 81-88.doi:dx.doi.org/10.1016/j.jphotobiol.2009.01.002

Sudhamalla, B., Gokara, M., Ahalawat, N., Amooru, D. G. & Subramanyam, R. (2010). Molecular dynamics simulation and binding studies of β-sitosterol with human serum albumin and its biological relevance. The Journal of Physical Chemistry B 114: 9054-9062.doi:dx.doi.org/10.1021/jp102730p

Sudlow, G., Birkett, D. & Wade, D. (1976). Further characterization of specific drug binding sites on human serum albumin. Molecular Pharmacology 12: 1052-1061.

Sudlow, G., Birkett, D. J. & Wade, D. N. (1975). The characterization of two specific drug binding sites on human serum albumin. Molecular Pharmacology 11: 824-832.

Sunshine, A. & Laska, E. (1975). Nefopam and morphine in man. Clin Pharmacol Ther 18: 530-534.doi:dx.doi.org/10.1002/cpt1975185part1530

Tabachnick, M. (1964). Thyroxine-protein interactions I. Binding of thyroxine to human serum albumin and modified albumins. Journal of Biological Chemistry 239: 1242-1249. Retrived from http://www.jbc.org/content/239/4/1242.long

Tayeh, N., Rungassamy, T. & Albani, J. R. (2009). Fluorescence spectral resolution of tryptophan residues in bovine and human serum albumins. Journal of Pharmaceutical and Biomedical Analysis 50: 107-116.doi:dx.doi.org/10.1016/j.jpba.2009.03.015

Tigerstedt, I., Sipponen, J., Tammisto, T. & Turunen, M. (1977). Comparison of nefopam and pethidine in postoperative pain. Br J Anaesth 49: 1133-1138. doi:dx.doi.org/10.1093/bja/49.11.1133

van de Weert, M. & Stella, L. (2011). Fluorescence quenching and ligand binding: A critical discussion of a popular methodology. Journal of Molecular Structure 998: 144-150. doi:dx.doi.org/10.1016/j.molstruc.2011.05.023

van Gunsteren, W. F., Billeter, S. R., Eising, A. A., Hünenberger, P. H., Krüger, P., Mark, A. E., Scott, W. R. & Tironi, I. G. (1996). Biomolecular Simulation: The {GROMOS96} manual and user guide. Retrived from https://books.google.co.in/books/about/Biomolecular_Simulation.html?id=0TbJAAAACAAJ&redir_esc=y

Van Gunsteren, W. F., Daura, X. & Mark, A. E. (1998). GROMOS force field. Encyclopedia of computational chemistry 2: 1211–1216. doi: 10.1002/0470845015.cga011

Varshney, A., Sen, P., Ahmad, E., Rehan, M., Subbarao, N. & Khan, R. H. (2010). Ligand binding strategies of human serum albumin: how can the cargo be utilized? Chirality 22: 77-87. doi:dx.doi.org/10.1002/chir.20709

Yeggoni, D. P., Gokara, M., Manidhar, D. M., Rachamallu, A., Nakka, S., Reddy, C. S. & Subramanyam, R. (2014). Binding and molecular dynamics studies of 7-hydroxycoumarin derivatives with human serum albumin and its pharmacological importance. Mol Pharm 11: 1117-1131.doi:dx.doi.org/10.1021/mp500051f

Yeggoni, D. P., Rachamallu, A., Kallubai, M. & Subramanyam, R. (2015). Cytotoxicity and comparative binding mechanism of piperine with human serum albumin and alpha-1-acid glycoprotein. Journal of Biomolecular Structure and Dynamics 33: 1336-1351.doi:dx.doi.org/10.1080/07391102.2014.947326

Yeggoni, D. P. & Subramanyam, R. (2014). Binding studies of L-3,4-dihydroxyphenylalanine with human serum albumin. Mol Biosyst 10: 3101-3110.doi:dx.doi.org/10.1039/C4MB00408F

Zhang, G., Que, Q., Pan, J. & Guo, J. (2008). Study of the interaction between icariin and human serum albumin by fluorescence spectroscopy. Journal of Molecular Structure 881: 132-138.doi:dx.doi.org/10.1016/j.molstruc.2007.09.002

Zsila, F. (2013). Subdomain IB Is the Third Major Drug Binding Region of Human Serum Albumin: Toward the Three-Sites Model. Molecular Pharmaceutics 10: 1668-1682. doi:dx.doi.org/10.1021/mp400027q

Zsila, F., Bikádi, Z. & Simonyi, M. (2003). Probing the binding of the flavonoid, quercetin to human serum albumin by circular dichroism, electronic absorption spectroscopy and molecular modelling methods. Biochemical Pharmacology 65: 447-456.doi:dx.doi.org/10.1016/S0006-2952(02)01521-6

Zunszain, P. A., Ghuman, J., Komatsu, T., Tsuchida, E. & Curry, S. (2003). Crystal structural analysis of human serum albumin complexed with hemin and fatty acid. BMC Structural Biology 3: 1-9.doi:dx.doi.org/10.1186/1472-6807-3-6

Scheme 1. Structure of Nefopam Analogues

1. 6-(phenyl)-7-methyl-9 ethyl 5, 6-dihydro-2H- benzo[b] [1, 4] oxazocine-8-carboxylic acid ethyl ester Nefopam analogue 1 (NF1). 2. 9-(4-chloro phenyl)-6-(4-hydroxy phenyl)-7-methyl-5, 6-dihydro-2H-benzo[b] [1, 4] oxazocine-8-carboxylic acid ethyl ester Nefopam analogue 2 **(NF2)**. (**NF2**). 3. 6-(4-hydroxy phenyl)-7-methyl-9-propyl-5, 6-dihydro-2H benzo[b] [1, 4] oxazocine-8-carboxylic acid ethyl ester Nefopam analogue 3 **(NF3).**

Figure 1. Fluorescence emission spectra of Nefopam analogues with HSA in 0.1M phosphate buffer pH 7.2, λ_{ex} = 285 nm. λ_{em} = 362 nm. (A) Free HSA (0.001 mM) and free HSA with different concentrations of NF1 (0.001-0.009 mM), (A1)Modified Stern-Volmer plot HSA-NF1 complex (B) Free HSA (0.001 mM) and free HSA with different concentrations of NF2 (0.001-0.009 mM), (B2) Modified Stern-Volmer plot HSA-NF2 complex (C) Free HSA (0.001 mM) and free HSA with different concentrations of NF3 (0.001-0.009 mM), (C1)Modified Stern-Volmer plot HSA-NF3 complex

Figure 2.CD spectra of the free HSA and Nefopam analogues with HSA. (A) HSA and HSA-NF1 complexes in aqueous solution with an HSA concentration of 0.001 mM and NF1 concentrations were 0.001, 0.005 and 0.009 mM (B) HSA and HSA-NF2 complexes in aqueous solution with an HSA concentration of 0.001 mM and NF2 concentrations were 0.001, 0.005 and 0.009 mM. (C) HSA and HSA-NF3 complexes in aqueous solution with an HSA concentration of 0.001 mM and NF3 concentrations were 0.001, 0.005 and 0.009 mM.

Figure 3.Spectra of Secondary Structure (Percentage %) free HSA and Nefopam analogues with HSA; with an HSA concentration of 0.001 mM and NF's concentrations were 0.001, 0.005 and 0.009 mM.

Figure 4. Docking conformation of N1-HSA complex obtained from Autodock v 4.2. (A) N1 bound to IIIA domain on HSA (Protein represented in ribbon model and ligand represented in stick model) (B) Stereo view of N1 bound to subdomain IIIA on HSA (prepared by using pymol v 1.5) in which N1 is rendered as capped sticks and surrounding residues as lines (2 hydrogen bonds with LYS 413) (C) The hydrophobic pocket of IIIA domain surrounding the N1. (D) N2 bound to IB domain on HSA (Protein represented in ribbon model and ligand represented in stick model) (E) Stereo view of N2 bound to subdomain IB on HSA (prepared by using pymol v 1.5) in which N2 is rendered as capped sticks and surrounding residues as lines (F) The hydrophobic pocket of IB domain surrounding the N2.(G) N3 bound to IIA domain on HSA (Protein represented in ribbon model and ligand represented in stick model) (H) Stereo view of N3 bound to subdomain IIA on HSA (prepared by using pymol v 1.5) in which N3 is rendered as capped sticks and surrounding residues as lines (I) The hydrophobic pocket of IIA domain surrounding the N3.

Figure 5. RMSD *vs* Time (ns) plot of Nefopam analogues with has (A) Plot of RMSD of C–Cα–N backbone vs simulation for solvated HSA and HSA + NF1 complexes during 10 ns. (B) Plot of RMSD of C–Cα–N backbone vs simulation for solvated HSA and HSA + NF2 complexes during 10 ns (C) Plot of RMSD of C–Cα–N backbone vs simulation for solvated HSA and HSA + NF3 complexes during 10 ns.

Figure 6. Rg *vs* Time (ns) Plot of Nefopam analogues with HSA (A) *R*g values during 10ns of MD simulation of HSA and NF1 complex. (B) *R*g values during 10 ns of MD simulation of HSA and NF2 complex. (C) *R*g values during 10 ns of MD simulation of HSA and NF3 complex.

Figure 7. RMSF vs Residue number over 10 (ns), Plot of Nefopam analogues with HSA (A) *R*MSF values during 10ns of MD simulation of HSA and NF1 complex. (B) *R*MSF values during 10 ns of MD simulation of HSA and NF2 complex. (C) *R*MSF values during 10 ns of MD simulation of HSA and NF3 complex.

Scheme 1. Structure of Nefopam analogues (NF1, NF2 and NF3)

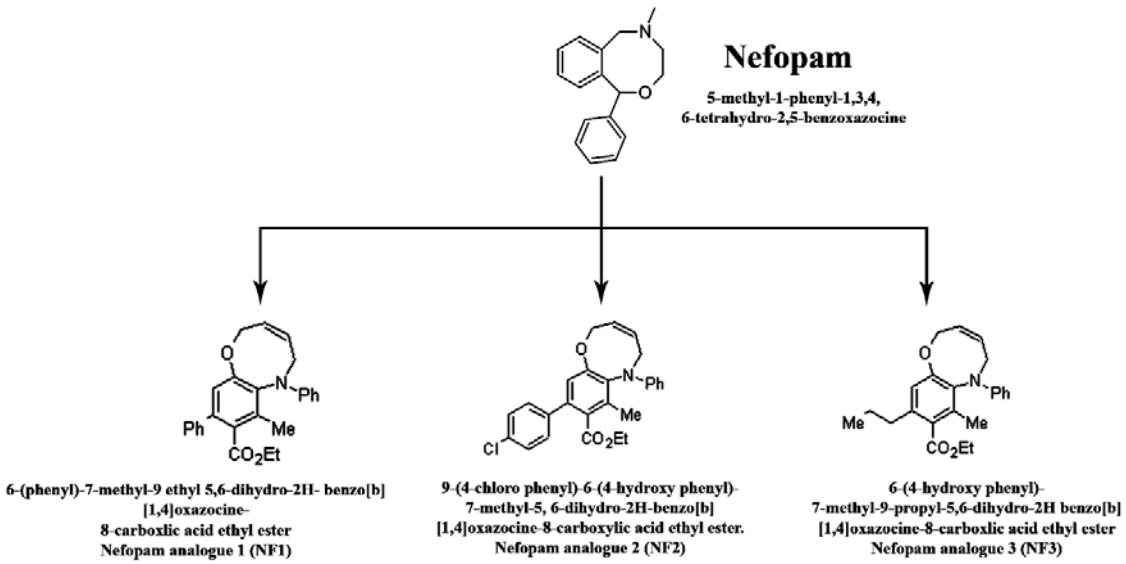

Figure 1.

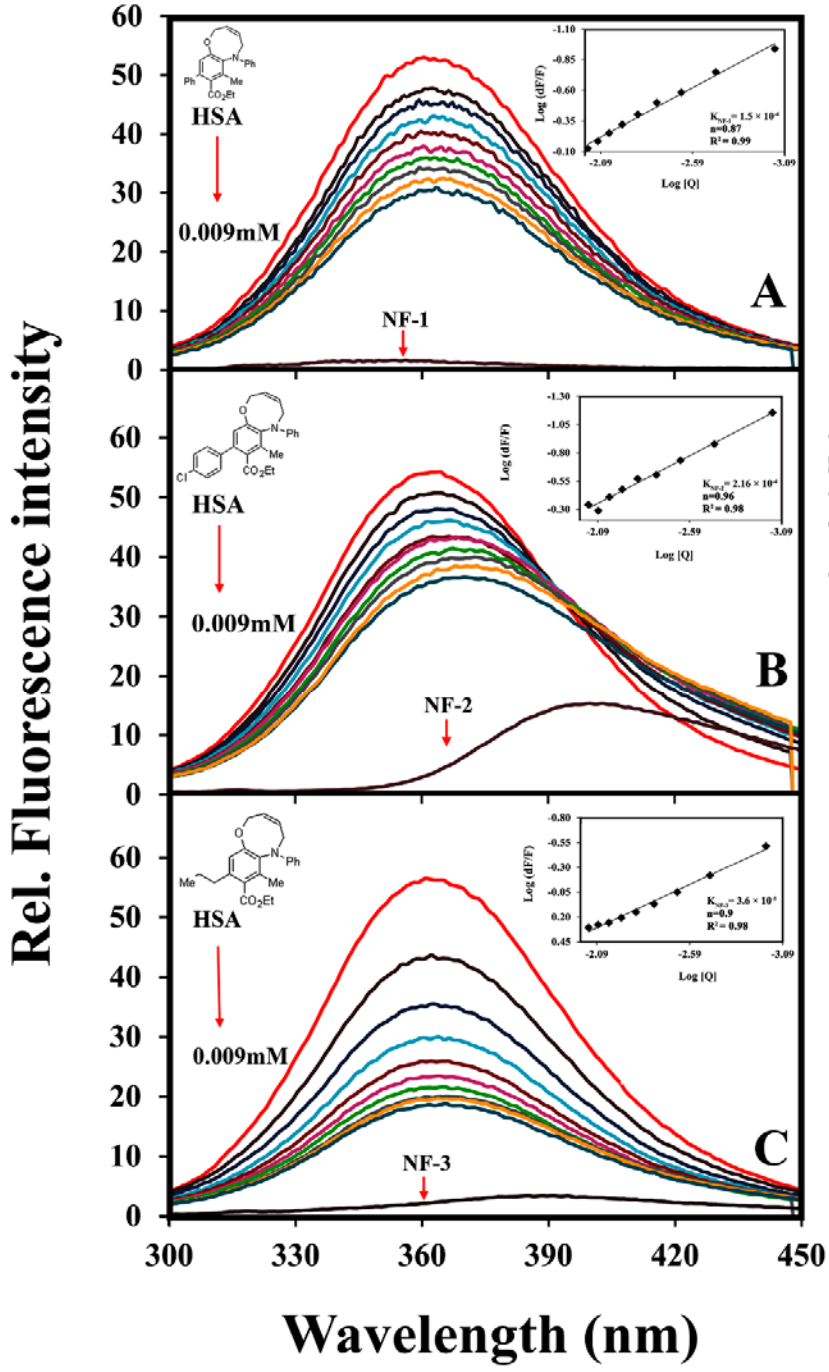

Figure 2.

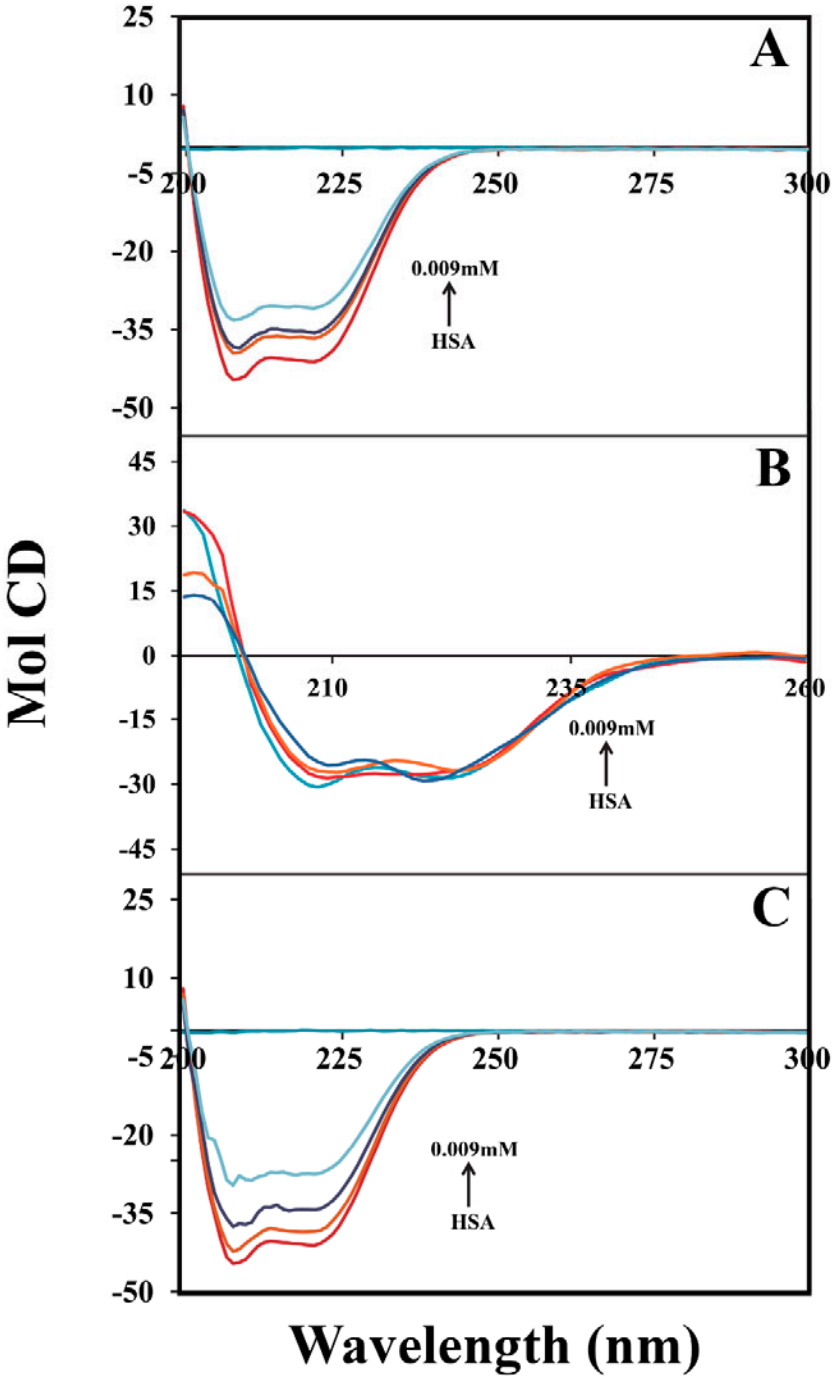

Figure 3.

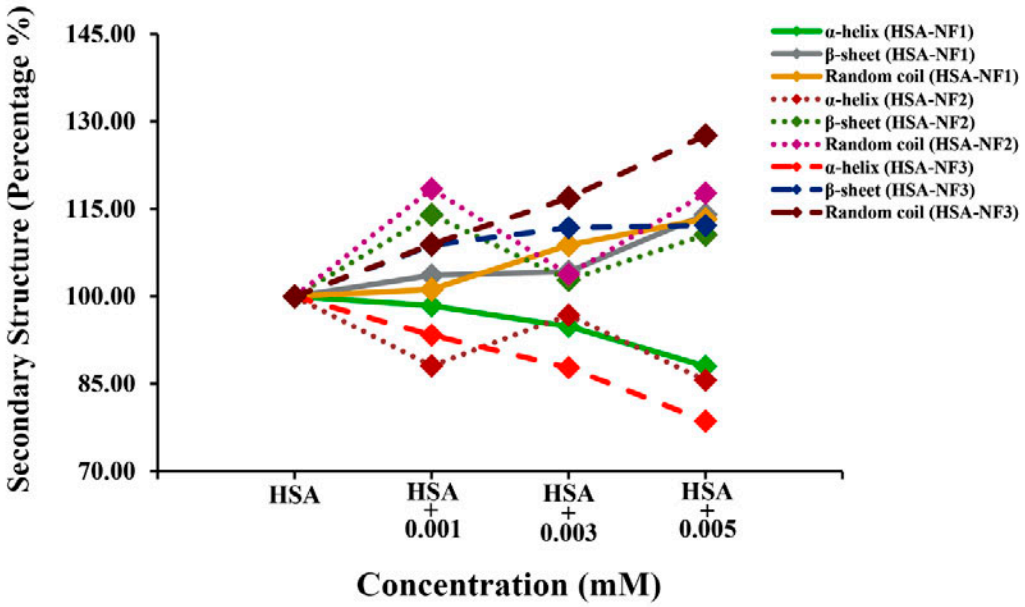

Figure 4.

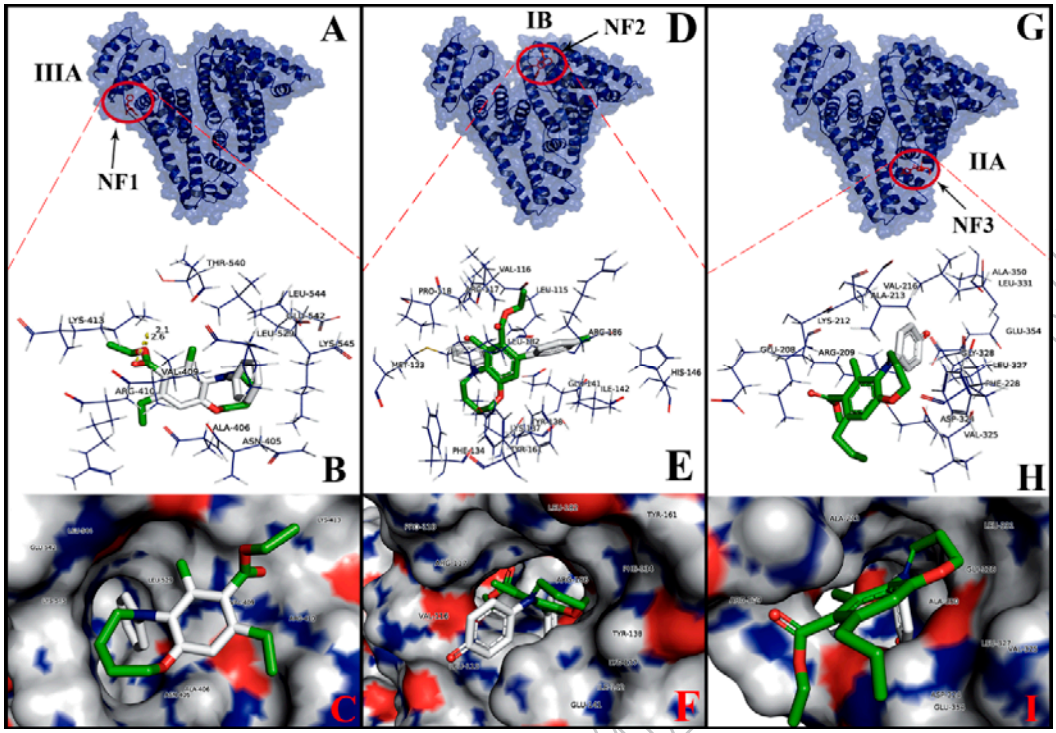

Figure 5.

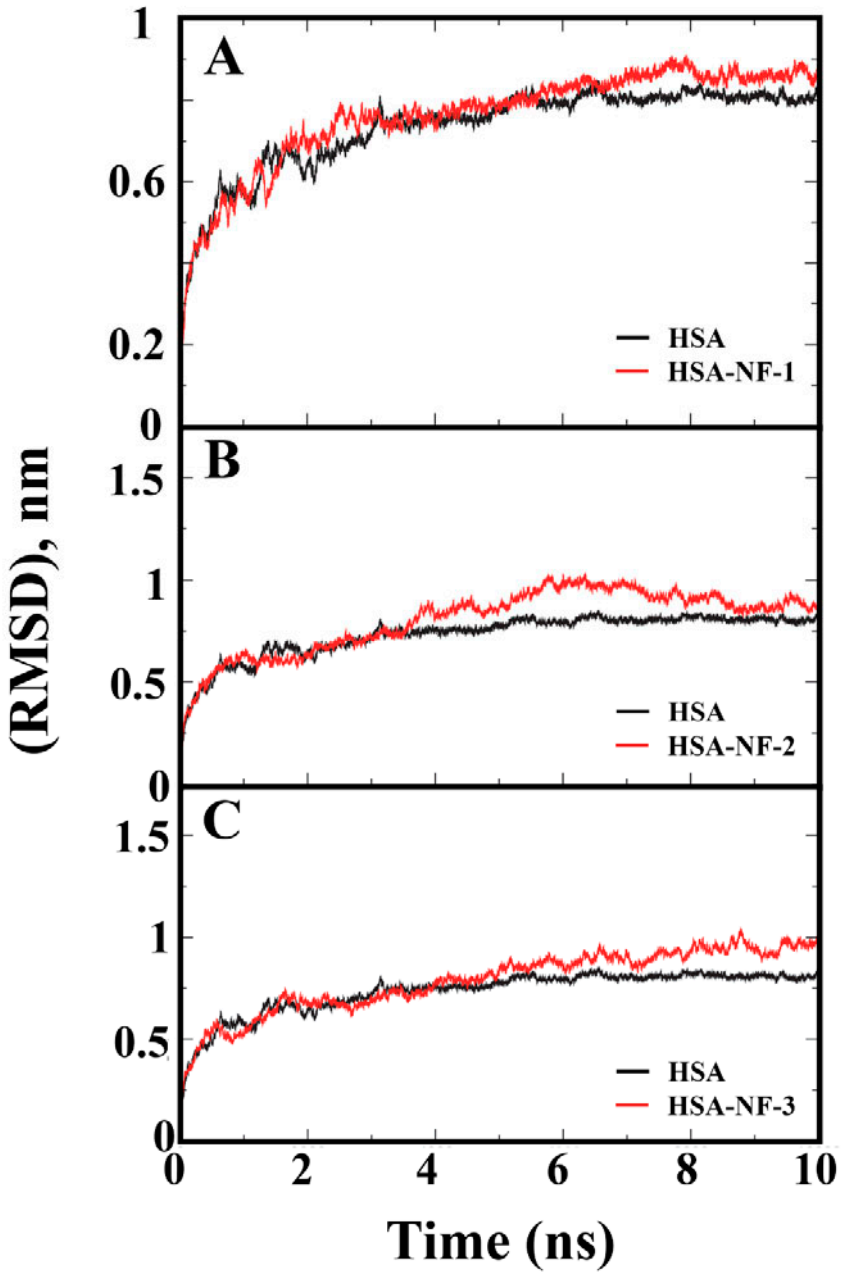

Figure 6.

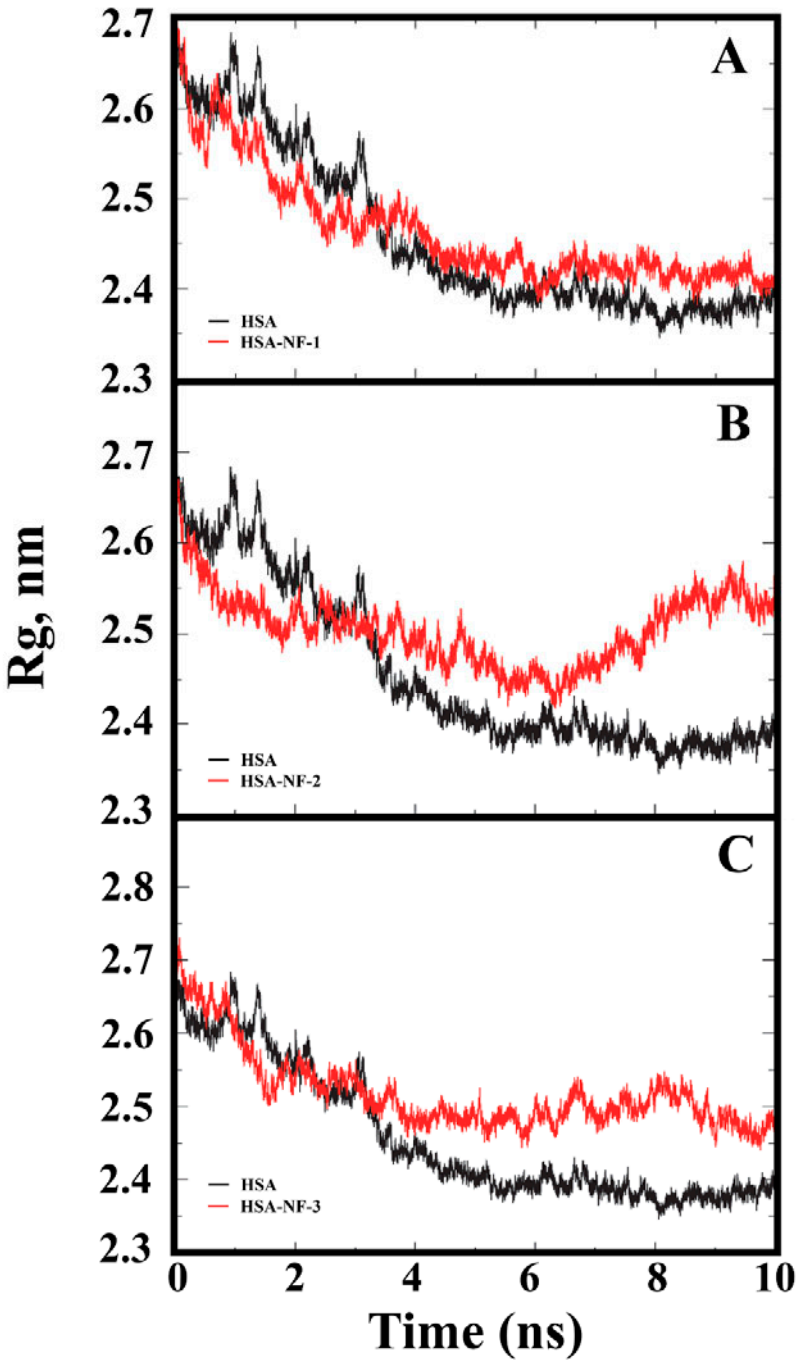

Figure 7.

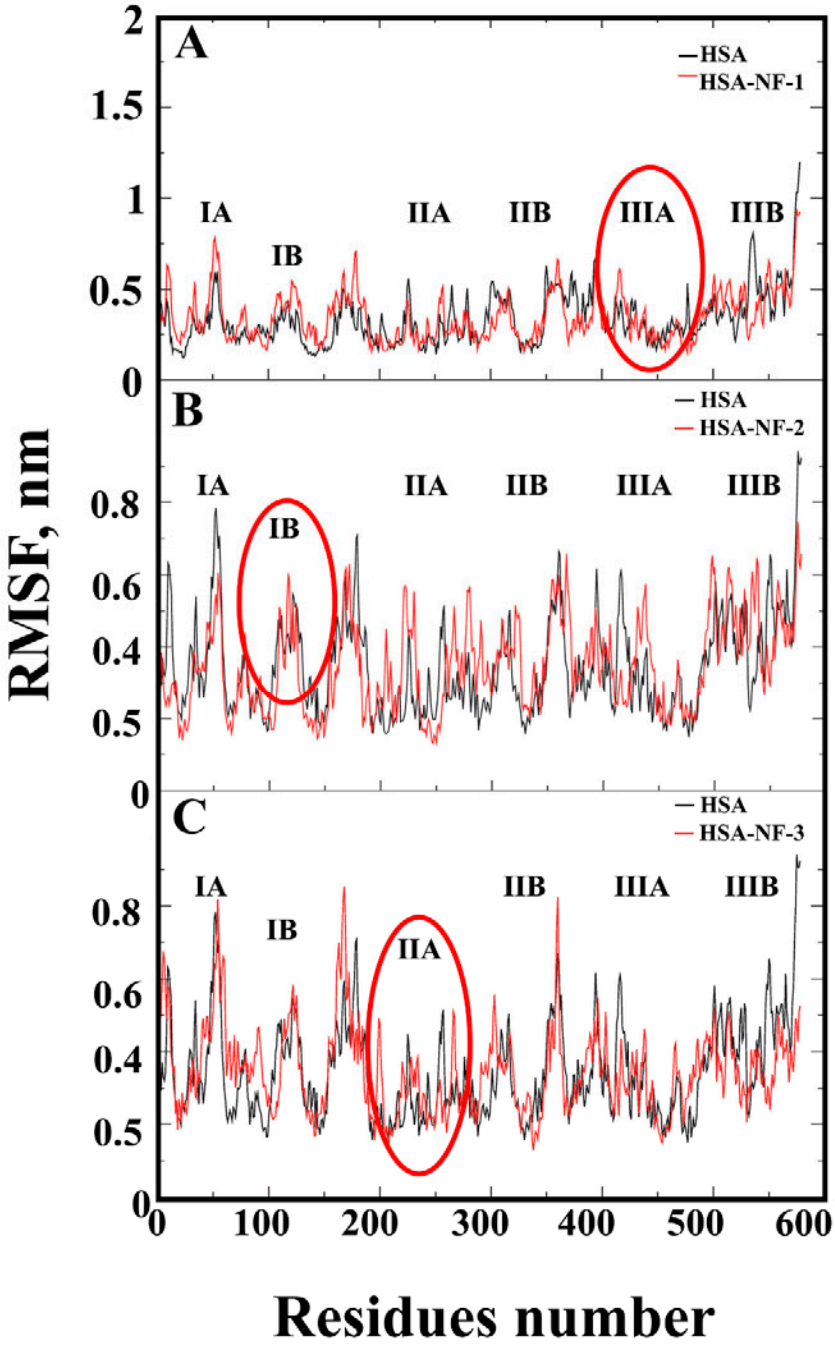

Table 1: Binding constants of Nfs with HSA obtained from fluorescence data and also, binding constants with site marks.

S.No	Analogues (M^{-1})		Site Markers (M^{-1})	
1	NF1	$1.53 \pm 0.057 \times 10^4$	Ibuprofen	$9.3 \pm 0.1 \times 10^5$
2	NF2	$2.16 \pm 0.071 \times 10^4$	Lidocaine	$1.02 \pm 0.1 \times 10^4$
3	NF3	$3.6 \pm 0.102 \times 10^5$	Phenylbutazone	$1.4 \pm 0.102 \times 10^5$

Supplementary data

Figure S1

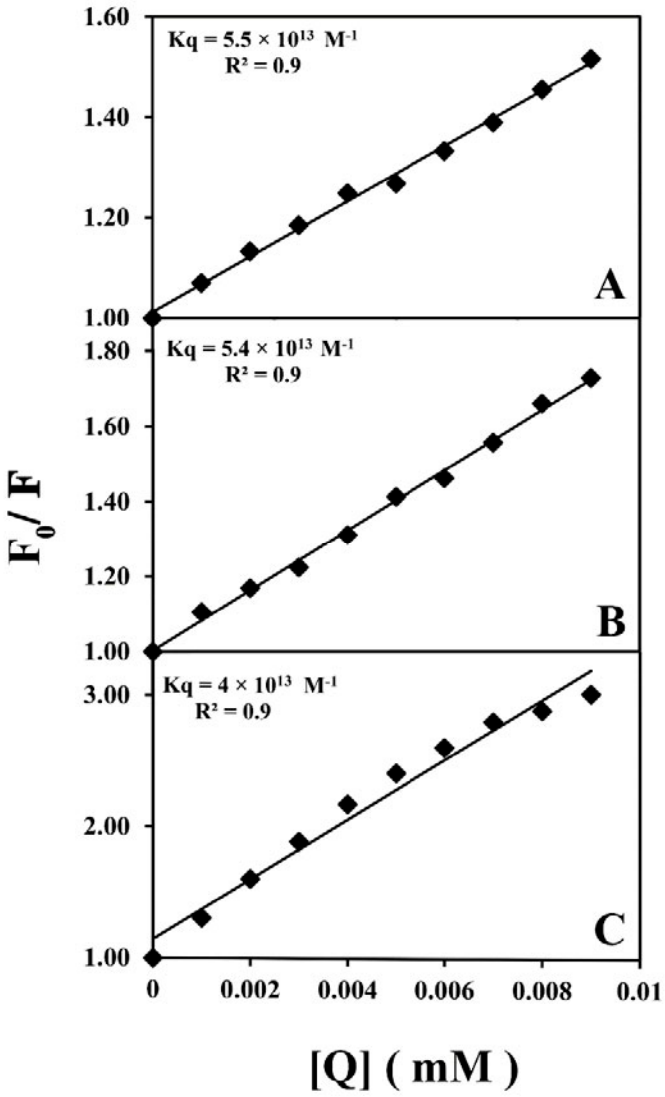

Figure S1.

Stern–Volmer plots of bimolecular quenching constants (Kq) of Nefopam analogues with HSA complexes at different concentrations of nefopam analogues used to determine static and dynamic quenching mechanism. (A) NF1–HSA, (B) NF2–HSA, and (C) NF3–HSA.

Figure S2. Schematic representation of Nefopam analogues with replaced R-groups.

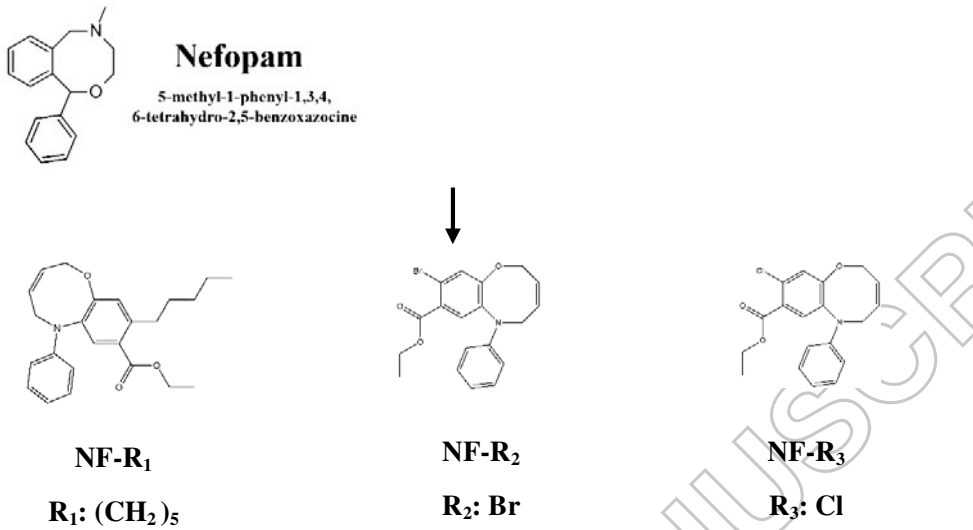

Figure S3.

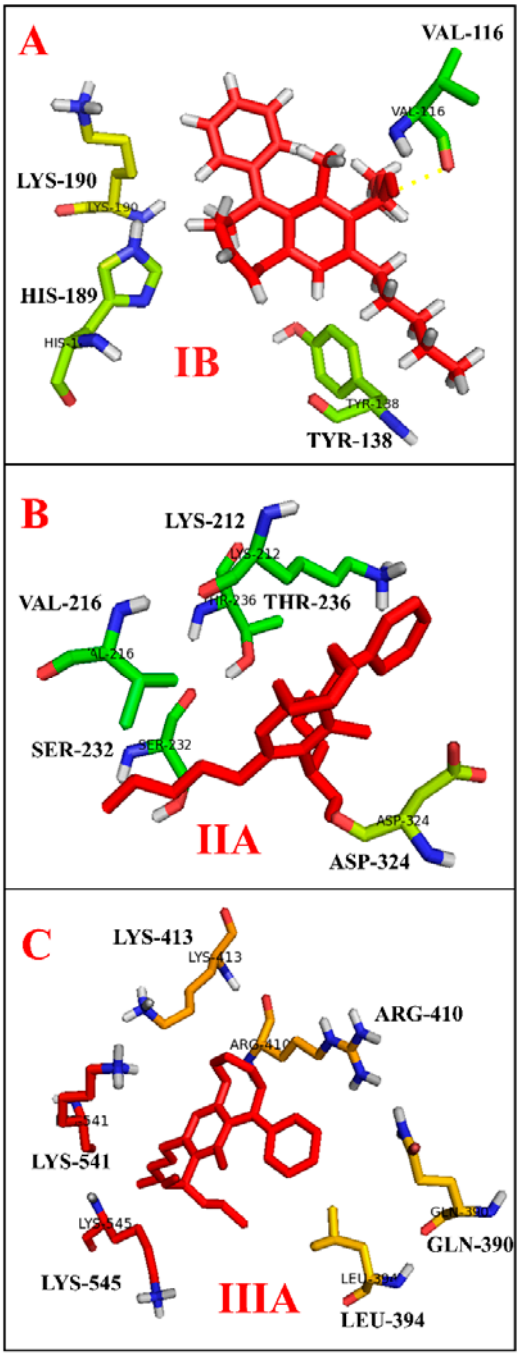

Figure S3. Docking conformation of NF-R_1 -HSA complex with three binding sites i.e., IB, IIA and IIIA. (A) NF-R_1 bound to IB, (B) NF-R_1 bound to IIA (C) NF-R_1 bound to IIIA. Note: R1 $(CH_2)_5$

Figure S4

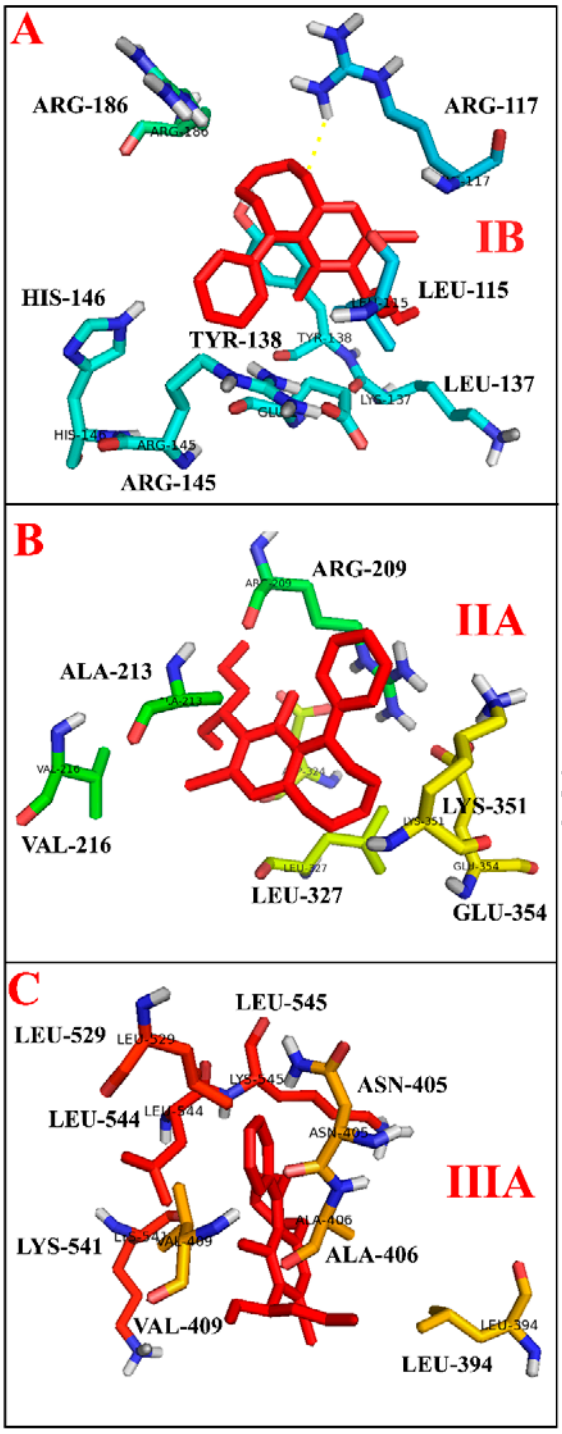

Figure S4. Docking conformation of NF-R_2 -HSA complex with three binding sites i.e., IB, IIA and IIIA. (A) NF-R_2 bound to IB, (B) NF-R_2 bound to IIA (C) NF-R_1 bound to IIIA. Note: R2 **(Br).**

Figure S5

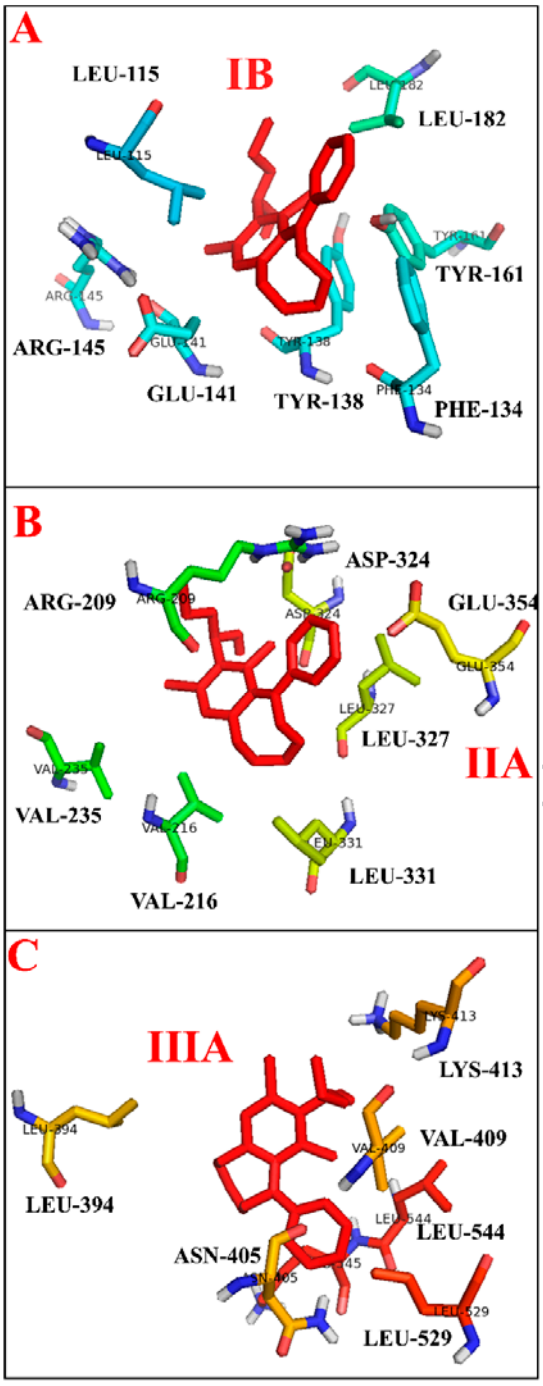

Figure S5. Docking conformation of NF-R_3 -HSA complex with three binding sites i.e., IB, IIA and IIIA. (A) NF-R_3 bound to IB, (B) NF-R_3 bound to IIA (C) NF-R_3 bound to IIIA. Note R3 (Cl).

S Table 1 Percentage of Secondary structural elements of the free HSA and NF's-HSA (NF1, NF2 and NF3) complexes. Mean SE ± (n=3)

Secondary structure (%)	HSA	HSA-0.001mM	HSA-0.005mM	HSA-0.009mM
HSA-NF1				
α-Helix	57.2±2.5	56.3±2.5	53.4±3.5	47±2.5
β-Sheet	25±0.8	25.96±1.2	27±0.9	30.8±1
Random coils	17.8±1.0	18.01±1.5	19.6±1.7	22.2±1.2
HSA-NF2				
α-Helix	57.1±2.5	50.3±2.2	48.7±2.12	41.7±1.82
β-Sheet	25±0.9	28.5±0.9	29.3±0.95	32.4±1.02
Random coils	17.9±1.8	21.2±2.1	22±2.22	25.9±2.6
HSA-NF3				
α-Helix	57.1±2.5	53.3±2.3	46.8±2.05	36.8±1.6
β-Sheet	25±0.88	27.2±0.74	30.4±0.98	34.1±1.07
Random coils	17.9±1.82	19.5±1.97	22.8±2.31	29.1±2.94

S Table 2: Comparative binding constants and free energies of NF-R1, NF-R2 and NF-R3 and Nefopham analogues (NF1, NF2, NF3).

Nefopham Analogues	**Binding Constant (M^{-1})**	**ΔG (kcal mol^{-1})**	**Nefopham analogues**	**Binding Constant (M^{-1})**	**ΔG (kcal mol^{-1})**
NF-R1	$1.40 \pm 0.062 \times 10^4$	-5.6	NF2	$2.16 \pm 0.071 \times 10^4$	-5.7
NF-R1	$1.71 \pm 0.046 \times 10^5$	-7.1	NF3	$3.6 \pm 0.102 \times 10^5$	-7.5
NF-R1	$6.03 \pm 0.054 \times 10^3$	-5.1	NF1	$1.53 \pm 0.057 \times 10^4$	-5.48
NF-R1	$1.00 \pm 0.021 \times 10^4$	-5.4	NF2	$2.16 \pm 0.071 \times 10^4$	-5.7
NF-R2	$1.16 \pm 0.072 \times 10^5$	-6.9	NF3	$3.6 \pm 0.102 \times 10^5$	-7.5
NF-R2	$5.56 \pm 0.081 \times 10^3$	-5.0	NF1	$1.53 \pm 0.057 \times 10^4$	-5.48
NF-R3	$1.15 \pm 0.05 \times 10^4$	-5.5	NF2	$2.16 \pm 0.071 \times 10^4$	-5.7
NF-R3	$1.02 \pm 0.044 \times 10^5$	-6.8	NF3	$3.6 \pm 0.102 \times 10^5$	-7.5
NF-R3	$4.47 \pm 0.05 \times 10^3$	-4.9	NF1	$1.53 \pm 0.057 \times 10^4$	-5.48